Role of dynamical deformation in pre-scission neutron multiplicity

Neeraj Kumar, Shabnam Mohsina, Jhilam Sadhukhan, and Shashi Verma

Role of dynamical deformation in pre-scission neutron multiplicity

Neeraj Kumar,[1] Shabnam Mohsina,[2,3] Jhilam Sadhukhan,[2,3] and Shashi Verma[1]

[1]*Department of Physics & Astrophysics, University of Delhi, Delhi-110007, INDIA*
[2]*Physics Group, Variable Energy Cyclotron Centre, Kolkata 700064, INDIA*
[3]*Homi Bhabha National Institute, Training School Complex, Anushakti Nagar, Mumbai 400094, INDIA*
(Dated: September 4, 2017)

The light-particle emission probability from an excited compound nucleus depends explicitly on the time-evolution of the system as the available internal excitation energy and, consequently, the particle decay widths depend on the instantaneous deformation of the nucleus. The Langevin dynamical model for fission is employed to extract this deformation dependence in pre-scission particle multiplicities by following the propagation of fissioning trajectories up to scission. The variation of particle decay widths with nuclear deformation is accounted more precisely in comparison to the existing calculations. The number of neutrons emitted from different configurations of the compound nucleus are calculated for a detailed analysis. The deformation dependence of particle emission widths is found to be relevant for highly fissile systems where the dynamics is primarily governed by the saddle to scission motion. This dynamical effect essentially predicts the nuclear shape evolution through evaporated light particles and, for a heavy compound system, simultaneous measurement of neutron multiplicities for fission and evaporation residue events can reveal its intricate nature.

PACS numbers: 24.10.-i, 25.85.-w, 25.70.Gh, 27.90.+b

I. INTRODUCTION

Precise calculation of neutron multiplicity in the process of nuclear fission is essential in many areas of basic and applied sciences. Neutron evaporation is one of the dominant decay mode in case of heavy-ion induced reactions. It is often used as the most effective probe to investigate nuclear properties like nuclear temperature [1, 2], level density [3, 4], fission lifetime [5–9], nuclear dissipation [10–16], etc. Moreover, in the contest of nuclear power production, neutron multiplicity plays the pivotal role in the operation of nuclear reactors. Considerable efforts has been devoted to measure the neutron multiplicity experimentally over a wide varieties of target-projectile combinations [7, 17–24]. However, theoretical refinements in the estimation of particle multiplicities has not been practiced much since it is first proposed in the seminal work by Weisskopf [25].

In statistical model calculations for fusion-fission reactions [12, 26], light particles and γ-rays are presumed to be evaporated from the spherical configuration of the compound nucleus (CN) and the associated decay widths are computed following this assumption. On an average, this consideration remains valid as long as the excited system evolves around the spherical configuration before it decays. The deformation dependence of decay widths is accounted approximately within the statistical model code JOANNE [27]. In this contest, present work plays a critical role to judge the applicability of statistical models for estimating the pre-scission particle multiplicities. In dynamical model calculations, decay widths are calculated at each time step of the fission trajectory [28, 29]. Here, although the available excitation energy is modified at each instant of time, the particle binding energies are not

usually adjusted in a coherent manner [30]. Therefore, the exact contribution emerging form this deformation dependence of decay widths is required to be extracted. Specifically, the saddle-to-scission dynamics often plays a decisive role in determining the pre-scission particle emission from a heavy CN [16, 31] and, in this region, the shift in particle multiplicities due to this deformation dependence is important to be analyzed.

In the present work, one dimensional Langevin dynamical model [9, 26] is utilized to study the pre-scission particle multiplicities. During the dynamical evolution, neutron (n), proton (p), α-particle, and γ-ray evaporations are considered within the Monte-Carlo method of random sampling [32]. The corresponding decay widths are evaluated at each time step with appropriate incorporation of its variation with nuclear deformation. Also, the calculations are performed with deformation-independent decay widths which are obtained for the spherical shape. Subsequently, we extracted the role of deformation dependence of decay probabilities in pre-scission particle multiplicities.

II. MODEL

The Funny-Hill parameter c [33] is used to describe the nuclear shape in one-dimensional collective space. Here, c defines the elongation of a CN. The Langevin equations governing the time propagation of c are given by [9]

$$\frac{dp}{dt} = -\frac{p^2}{2}\frac{d}{dc}\left(\frac{1}{\mathcal{M}}\right) - \frac{dF}{dc} - \eta\frac{p}{\mathcal{M}} + g\Gamma(t)$$
$$\frac{dc}{dt} = \frac{p}{\mathcal{M}} \tag{1}$$

where p represents momentum conjugate to c, $\mathcal{M}$ is the collective inertia calculated using the Warner-Wheeler prescription [34, 35] for incompressible and irrotational flow of nuclear fluid. The reduced dissipation strength $\beta = \eta/\mathcal{M}$ is considered as a free parameter [36]. The product $g\Gamma(t)$ is the random force with $\Gamma(t)$ being a time-dependent stochastic variable with the Gaussian distribution, and g is the strength of the random force that obeys the fluctuation-dissipation theorem: $g^2 = \eta T$. The temperature T (in MeV) is calculated from the ground state excitation energy E_{gs}^* of the CN as $T = \sqrt{E_{gs}^*/a_{gs}}$. The a_{gs} is the ground state value of the shape-dependent level density parameter $a(c)$ which is calculated following the Ref. [37]. Also, $a(c)$ is corrected for the nuclear shell effects as prescribed by Ignatyuk *et al.* [38]. The driving force is obtained from the Helmoltz free energy: $F(\ell,c) = V(\ell,c) - (a(c) - a_0)T^2$, where a_0 is the value of $a(c)$ at the spherical configuration. The liquid drop model potential energy $V(\ell,c)$ is calculated from the Yukawa-plus-exponential double folding procedure [39]. A phenomenological deformation dependent shell correction is added to $V(\ell,c)$ by following the procedure given in [40]. Also, $V(\ell,c)$ is corrected for the collective rotational energy of the CN having initial angular momentum ℓ. The excitation energy E^* of the CN is calculated by subtracting the experimental Q-value of the reaction V_Q and $V(c)$ from the center-of-mass energy $E_{c.m.}$ as

$$E^*(\ell,c) = E_{c.m.} - V_Q - V(\ell,c). \tag{2}$$

The statistical theory of Weisskopf is employed to calculate the partial decay width $\Gamma_\nu(\ell,c)$ corresponding to the emission of a light particle of type ν from the deformed CN with deformation c. The expression for $\Gamma_\nu(\ell,c)$ is given by [26],

$$\Gamma_\nu(\ell,c) = \frac{N_\nu}{\rho_{CN}(E^*(\ell,c))} \int_0^{E'(\ell,c)} de_\nu \rho_R(E'(c) - e_\nu)e_\nu \sigma_{inv}(e_\nu) \tag{3}$$

where, N_ν is a constant that depends solely on the type of the light particle and e_ν represents the kinetic energy of the emitted particle. σ_{inv} is the cross section for the inverse reaction [41, 42] and ρ_R (ρ_{CN}) is the density of states of the residual nucleus (CN) calculated using the Fermi gas model for nucleus [43, 44]. In the above equation, $E'(\ell,c) = E^*(\ell,c) - B_\nu(c) - \Delta E_{rot}$, where $B_\nu(c)$ is the binding energy of the emitted particle, and ΔE_{rot} is the change of the rotational energy due to the angular momentum carried away by the rotating particle. The particle binding energies $B_\nu(c)$ can be written as, $B_\nu(c) = M_\nu + M_R - M_{CN} + D_R(c) - D_{CN}(c)$ [27, 40]. Here, M_R (M_{CN}) is the mass of the daughter nucleus (CN), M_ν is the mass of the emitted particle, and $D_R(c)$ ($D_{CN}(c)$) denotes the deformation energy of the daughter nucleus (CN) at a particular deformation c. In the present work, experimental masses (M_R and M_{CN}) are used to calculate $B_\nu(c)$. Usually, dynamical
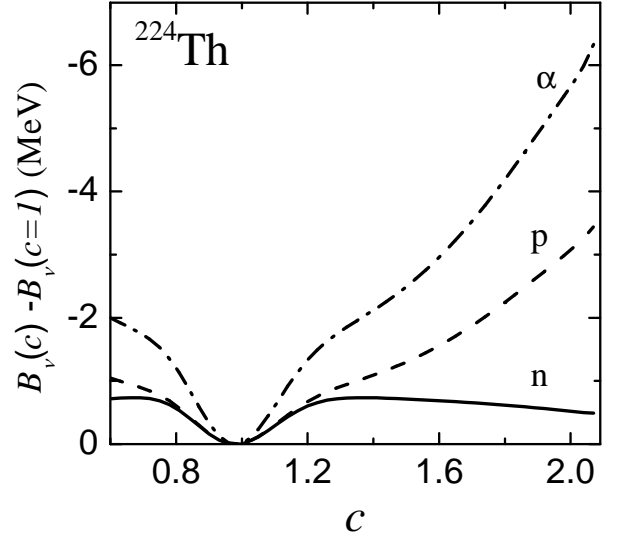

FIG. 1. Relative variation of neutron (solid line), proton (dashed line), and α-particle (dash-dotted line) binding energies with respect to the value at spherical shape ($c = 1$).

calculations are often combined with a subsequent statistical model calculation [26, 32, 45–47] due to computational limitations. Nevertheless, the motivation in this work is to distinguish the deformation of a CN for each of the particle and γ decay. Therefore, it is necessary to trace the complete trajectory of the system in small time steps with the help of a dynamical model code. To fulfill this requirement, we set the total dynamical time to a sufficiently large value (50,000 $\hbar$/MeV for the ^{16}O+^{208}Pb reaction at $E_{c.m.} \geq 100$ MeV) such that there is hardly any particle evaporation in the following statistical model part. Moreover, we have checked that the results relevant to the present study are insensitive to the coupling with the statistical model.

III. RESULTS

We first study the ^{16}O+^{208}Pb→^{224}Th reaction since the experimental values of pre-scission neutron multiplicities, n_{pre}, are well established for this system. For completeness, the variation of $B_\nu(c)$ with deformation c is shown in Fig. 1 for $\nu \equiv n$, p, and α. As found in [27], the binding energy of p and α changes substantially with deformation in comparison to the binding energy of n. It predicts a stronger impact of deformation dependence on Γ_p and Γ_α in respect to Γ_n. However, presently we focus only on the neutron multiplicities. We calculate n_{pre} for the above mentioned reaction with a constant $\beta = 3.5$MeV/$\hbar$. The justification for using a constant β is given in an earlier work [13]. In the upper panel of Fig. 2, the neutron multiplicities n_{pre}^+,
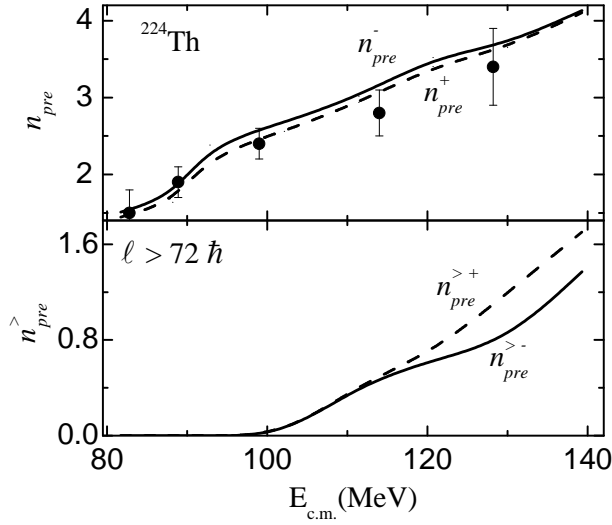
FIG. 2. Upper panel : n_{pre}^- (solid line) and n_{pre}^+ (dashed line) calculated with deformation independent $\Gamma_n(\ell, c = 1)$ and deformation dependent $\Gamma_n(\ell, c)$, respectively. Experimental values (solid circles) of n_{pre} is taken from [7]. Lower panel: $n_{pre}^{>-}$ (solid line) and $n_{pre}^{>+}$ (dashed line) calculated for $\ell \geq \ell_{crit}$ (see text).
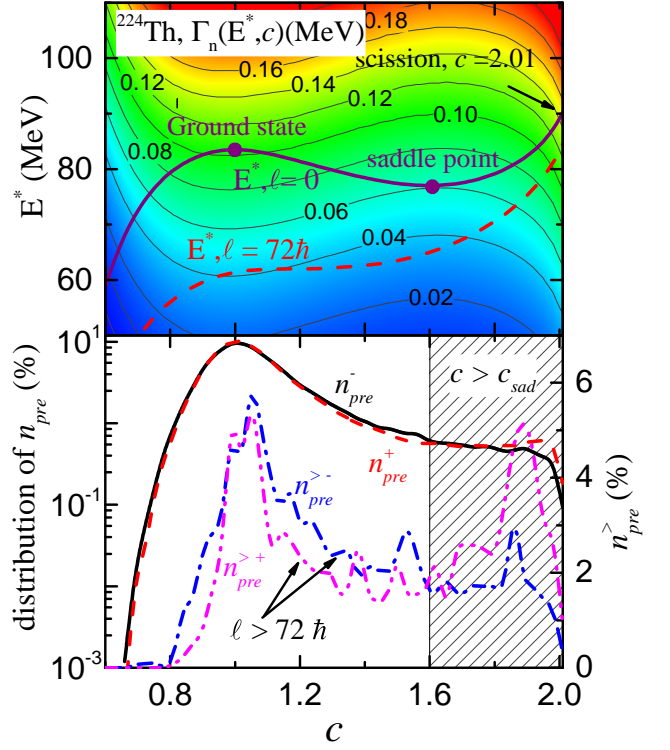

FIG. 3. (Color online) Upper Panel: Contours of $\Gamma_n(E^*, c)$ as a function of excitation energy and deformation for fixed $\ell = 0$. The $E^*(\ell, c)$ corresponding to $E_{c.m.} = 120$ MeV is shown for $\ell = 0$ (thick-solid line) and $\ell = 72\hbar$ (thick-dashed line). Lower panel: Distributions of n_{pre}^- (solid line) and n_{pre}^+ (dashed line) in log scale (left scale) and distributions of $n_{pre}^{>-}$ (dotted dashed line) and $n_{pre}^{>+}$ (double dotted-dashed-line) in linear scale (right scale) as functions of deformation c. The shaded belongs to the deformation larger than saddle-point deformation.

calculated with deformation dependent $\Gamma_n(\ell, c)$ (Eq. 3), are compared with the the neutron multiplicities n_{pre}^- obtained with the shape-independent $\Gamma_n(\ell, c = 1)$. Here, $c = 1$ corresponds to spherical shape. Also, the experimental values of n_{pre} are shown in this figure. As evident, n_{pre}^+ remains marginally smaller than n_{pre}^- at lower $E_{c.m.}$ and as the energy increases the difference becomes negligible. Next, in the lower panel of Fig. 2, we compare the neutron multiplicities $n_{pre}^{>+}$ and $n_{pre}^{>-}$ associated to fission events with $\ell \geq 72\hbar$. Here, '+' and '−' have the same meaning as defined in case of n_{pre}^+ and n_{pre}^-, respectively. The fission barrier of ^{224}Th vanishes at $\ell = 72\hbar$ (ℓ_{crit}, say). Hence, both the $n_{pre}^{>+}$ and $n_{pre}^{>-}$ are produced mostly during the fast saddle-to-scission transition. According to Fig. 2, this saddle-to-scission motion contributes in n_{pre} as $E_{c.m.}$ increases above 100 MeV. Moreover, $n_{pre}^{>+}$ becomes considerably higher than $n_{pre}^{>-}$ for $E_{c.m.} \geq 115$ MeV. All together we conclude that n_{pre} shows a contrasting behavior when the c-dependence in $\Gamma_n(\ell, c)$ is taken into account. It is suppressed at lower $E_{c.m.}$ where only smaller values of ℓ are populated. On the other hand, there is an enhancement in n_{pre}^+ as comparatively higher values of ℓ become abundant at a higher $E_{c.m.}$.

For a deeper understanding, we now demonstrate how $\Gamma_n(\ell, c)$ evolves along c for two distinct values of ℓ corresponding to same $E_{c.m.}$. At first, in Fig. 3 (upper panel), contours of $\Gamma_n(E^*, c)$ are plotted on a two-dimensional surface of E^* and c keeping ℓ constant at zero. For this plot, E^* is considered as a free parameter in Eq. 3 instead of using the actual

value given by Eq. 2. Next, the $E^*(\ell, c)$ of the ^{224}Th nucleus is calculated for $E_{c.m.} = 115$ MeV and shown in the same plot for $\ell = 0$ and ℓ_{crit}. The $\Gamma_n(\ell, c)$ at a particular ℓ can be determined from the intersections of a E^*-line with $\Gamma_n(E^*, c)$ contours. Here, the dependence of the $\Gamma_n(E^*, c)$ surface on ℓ can be neglected for the present schematic interpretation. Now, in fission process, neutrons are primarily evaporated from the collective space in between the ground state and scission configurations and, as evident from Fig. 3, the relative change in $\Gamma_n(\ell = \ell_{crit}, c)$ is more drastic in this region than $\Gamma_n(\ell = 0, c)$. Precisely, $\Gamma_n(\ell = 0, c)$ decreases from ~ 0.10 MeV to ~ 0.06 MeV as c changes from the ground state to saddle point (indicated by circular symbols in Fig. 3) and then rises to ~ 0.12 MeV at scission. In contrast, $\Gamma_n(\ell = \ell_{crit}, c)$ effectively increases by almost thrice of its ground state value as the system moves to scission. Also, in this case, the dynamics near scission is a principal component of the entire decay process since the system rolls down very fast in absence of a potential barrier. These arguments partly explain the deformation dependence of n_{pre}. Further, to justify
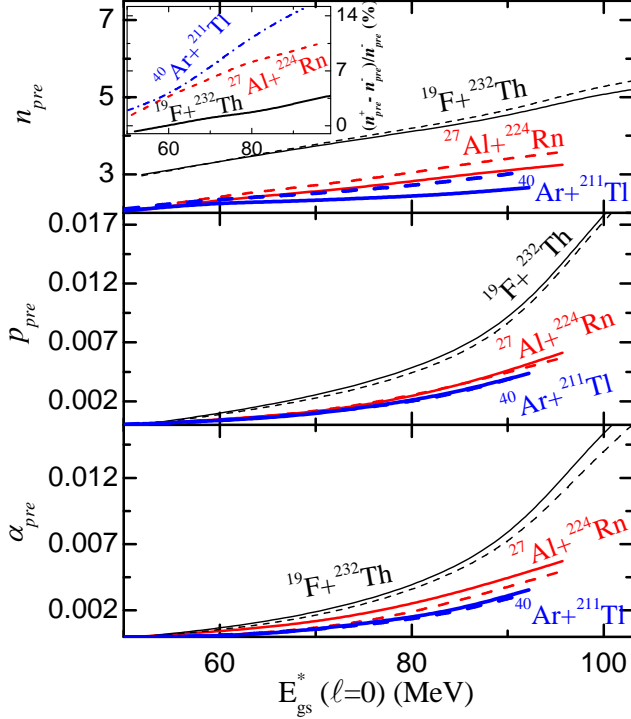
FIG. 4. (Color online) Pre-scission particle multiplicities for different target-projectile combinations calculated with (dashed lines) and without (solid lines) deformation dependence. Inset of top panel: n_{frac} (see text) as a function of excitation energy for these systems.
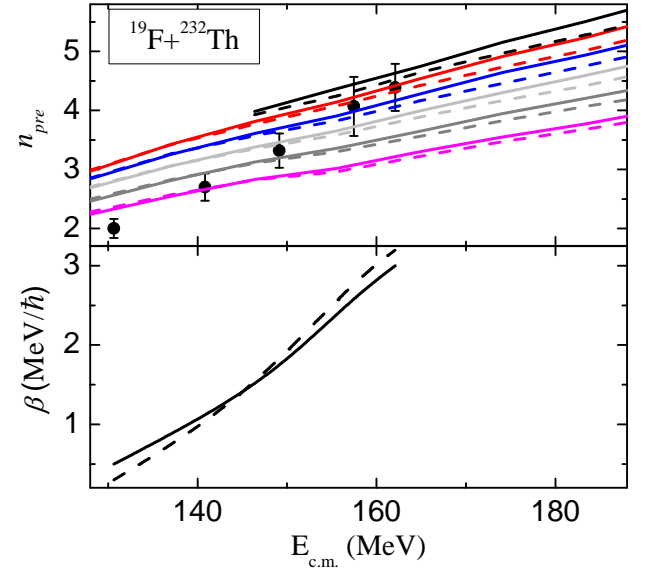

FIG. 5. Upper panel: (color online) n_{pre} as a function of excitation energy for deformation dependent (solid lines) and independent (dashed lines) neutron decay widths calculated for β=1.0,1.5, 2.0, 2.5, 3.0, and 3.5 (with n_{pre} smaller to larger). Experimental data points (solid circles) are from Ref. [48]. Lower panel: The excitation energy dependence of β for deformation dependent (solid line) and independent (dashed line) neutron decay widths.

the nature of n_{pre} in a more comprehensive manner, we have drawn the distributions of n_{pre} as a function of c in the lower panel of Fig. 3. $E_{c.m.} = 115$ MeV is chosen for this purpose as both the effects associated to high and low values of ℓ are noticeable (Fig. 2) at this energy. We see that n_{pre} is primarily contributed from c around the ground state configuration and, in this portion, n_{pre}^+ is slightly lower than n_{pre}^-. Also, similar behavior can be observed for the distributions of $n_{pre}^>$. Then, as the system becomes very deformed for $c > c_{sad}$, $n_{pre}^{>+}$ grows above $n_{pre}^{>-}$. This transition is visible in the cumulative spectrum of n_{pre} only when the partial contribution from higher ℓ becomes important at a specific $E_{c.m.}$.

The result for ^{224}Th gives the impetus to extend the analysis to heavier systems where the influence of $\ell \geq \ell_{crit}$ is more prominent, vis-a-vis the saddle-to-scission dynamics is relevant. To this end, we consider three different target-projectile combinations - (1) ^{19}F+^{232}Th, (2) ^{27}Al+^{224}Rn, and (3) ^{40}Ar+^{211}Tl. All these combinations produce the same CN ^{251}Es. However, for the same ground state excitation energy, combination (3) is produced at a higher ℓ in comparison to (2) and (1). Similarly the most-probable ℓ for (2) is higher than that in case of (1). Now, we can

conjecture that the deformation dependence of n_{pre} will be most prevailing in case of (3). We plot the pre-scission particle multiplicities (n_{pre}, p_{pre} and α_{pre}) for all the three combinations in Fig. 4. Also, the fractional increase in pre-scission neutron multiplicities, $n_{frac} = 100(n_{pre}^+ - n_{pre}^-)/n_{pre}^-$, is shown. As anticipated, there is a strong deformation depende nce in pre-scission
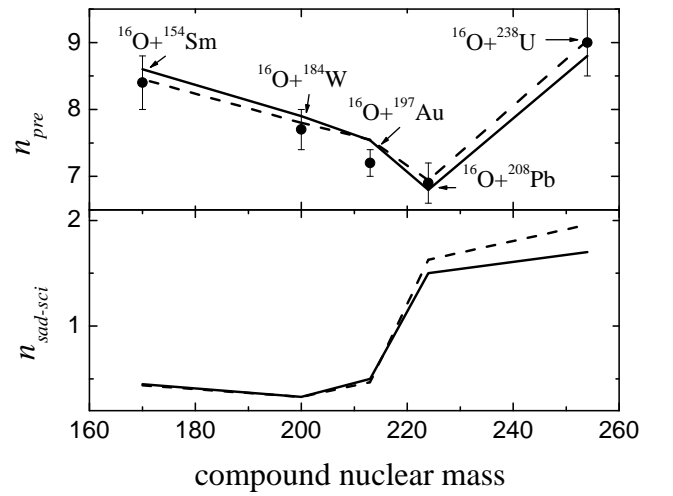

FIG. 6. Upper panel: n_{pre}^+ (dashed line) and n_{pre}^- solid line for different systems as indicated along with experimental data points (solid circles). Lower panel:Associated saddle to scission neutron multiplicity ($n_{sad-sci}$).

neutron multiplicity for the combinations (3) and (2). Even though the total neutron multiplicity is small for these two systems, the fractional increase n_{frac} is considerably greater than zero. A similar explanation holds for p_{pre} and α_{pre}: p_{pre}^+ (α_{pre}^+) increases and merges with p_{pre}^- (α_{pre}^-) as the mass asymmetry decreases. In fact, p and α are mainly evaporated at an earlier stage of the dynamics when considerable amount of excitation energy is available and the shape is nearly spherical. Therefore, the deformation effect is not very prominent and p_{pre}^+ (α_{pre}^+) remains lower than p_{pre}^- (α_{pre}^-) as found in case of n_{pre} for ^{224}Th. Also, we calculate the energy dependence of β for the combination (3) for which n_{pre} is measured experimentally. The n_{pre}^+ and n_{pre}^- calculated for different β are compared with experimental n_{pre} in Fig. 5 (upper panel). Then the energy dependences of β are extracted for both the '+' and '−' cases. It is plotted in the lower panel of Fig. 5. This dependence is revealed to be reduced when c-dependent $\Gamma_n(\ell,c)$ is considered. Although a constant energy independent β reproduces the experimental n_{pre} for ^{224}Th, it is inadequate in case of ^{251}Es as the fission barrier is small for this system.

In order to study the saddle to scission dynamics, we have also estimated the dynamical deformation dependency on saddle to scission motion using saddle to scission neutrons ($n_{sad-sci}$) as a probe for various experimentally measured systems, from Ref. [7]. The n_{pre} and $n_{sad-sci}$ are plotted in Fig. 6 for these systems. The initial excitation energy of the compound nuclei are 205.8, 195.8, 191.4, 187.3, and 191.9 in MeV for compound systems with atomic mass 170, 200, 213, 224, and 254, respectively. As expected, the n_{pre}^+ is enhanced when the saddle to scission motion contributes substantially. On the other hand, n_{pre}^- is larger than n_{pre}^+ for low fissility systems. We should mention that the experimental data on charged particle multiplicities are not reproduced as the effect due to deformation dependence is expected to be negligible.

IV. CONCLUSION

The role of nuclear deformation in determining the neutron decay width and its subsequent effect in pre-scission neutron multiplicity is investigated. A systematic analysis is presented to explore this dependence. Specifically, an enhancement in pre-scission neutron multiplicity due to this deformation dependence is predicted for the systems where the saddle-to-scission dynamics is crucial. This suggests that a precise calculation of the deformation dependence of particle emission widths must be incorporated within dynamical model for fission. Moreover, the dynamical effect discussed here can be verified by a simultaneous measurement of pre-scission neutron multiplicity and the evaporation residue neutron multiplicity which is mostly unaffected by saddle-to-scission dynamics.

V. ACKNOWLEDGEMENTS

[1] D. Hinde, Nucl. Phys. A **553**, 255 (1993).
[2] D. Mondal, D. Pandit, S. Mukhopadhyay, S. Pal, B. Dey, S. Bhattacharya, A. De, S. Bhattacharya, S. Bhattacharyya, P. Roy, K. Banerjee, and S. R. Banerjee, Phys. Rev. Lett. **118**, 192501 (2017).
[3] K. Banerjee, S. Bhattacharya, C. Bhattacharya, M. Gohil, S. Kundu, T. K. Rana, G. Mukherjee, R. Pandey, P. Roy, H. Pai, A. Dey, T. K. Ghosh, J. K. Meena, S. Mukhopadhyay, D. Pandit, S. Pal, and S. R. Banerjee, Phys. Rev. C **85**, 064310 (2012).
[4] P. Roy, K. Banerjee, C. Bhattacharya, R. Pandey, A. Sen, S. Manna, S. Kundu, T. K. Rana, T. K. Ghosh, G. Mukherjee, T. Roy, A. Dhal, A. Dey, J. K. Meena, A. K. Saha, D. Pandit, S. Mukhopadhyay, and S. Bhattacharya, Phys. Rev. C **94**, 064607 (2016).
[5] D. Hinde, D. Hilscher, and H. Rossner, Nucl. Phys. A **502**, 497 (1989).
[6] D. Hilscher, H. Rossner, B. Cramer, B. Gebauer, U. Jahnke, M. Lehmann, E. Schwinn, M. Wilpert, T. Wilpert, H. Frobeen, E. Mordhorst, and W. Scobel, Phys. Rev. Lett. **62**, 1099 (1989).
[7] D. J. Hinde, D. Hilscher, H. Rossner, B. Gebauer, M. Lehmann, and M. Wilpert, Phys. Rev. C **45**, 1229 (1992).
[8] Y. Aritomo, M. Ohta, T. Materna, F. Hanappe, O. Dorvaux, and L. Stuttge, Nucl. Phys. A **759**, 309 (2005).
[9] Y. Abe, S. Ayik, P.-G. Reinhard, and E. Suraud, Phys. Rep. **275**, 49 (1996).
[10] P. Grang and H. A. Weidenmller, Phys. Lett. B **96**, 26 (1980).

[11] P. Grangé, L. Jun-Qing, and H. A. Weidenmüller, Phys. Rev. C **27**, 2063 (1983).

[12] J. Sadhukhan and S. Pal, Phys. Rev. C **78**, 011603 (2008).

[13] J. Sadhukhan and S. Pal, Phys. Rev. C **81**, 031602 (2010).

[14] V. Singh, B. R. Behera, M. Kaur, A. Kumar, P. Sugathan, K. S. Golda, A. Jhingan, M. B. Chatterjee, R. K. Bhowmik, D. Siwal, S. Goyal, J. Sadhukhan, S. Pal, A. Saxena, S. Santra, and S. Kailas, Phys. Rev. C **87**, 064601 (2013).

[15] W. Ye, Phys. Rev. C **79**, 031601 (2009).

[16] N. Wang and W. Ye, Phys. Rev. C **87**, 051601 (2013).

[17] D. J. Hinde, R. J. Charity, G. S. Foote, J. R. Leigh, J. O. Newton, S. Ogaza, and A. Chatterjee, Phys. Rev. Lett. **52**, 986 (1984).

[18] A. Gavron, A. Gayer, J. Boissevain, H. Britt, J. Nix, A. Sierk, P. Grangé, S. Hassani, H. Weidenmller, J. Beene, B. Cheynis, D. Drain, R. Ferguson, F. Obenshain, F. Plasil, G. Young, G. Petitt, and C. Butler, Phys. Lett. B **176**, 312 (1986).

[19] D. Hinde, R. Charity, G. Foote, J. Leigh, J. Newton, S. Ogaza, and A. Chattejee, Nucl. Phys. A **452**, 550 (1986).

[20] W. P. Zank, D. Hilscher, G. Ingold, U. Jahnke, M. Lehmann, and H. Rossner, Phys. Rev. C **33**, 519 (1986).

[21] D. J. Hinde, H. Ogata, M. Tanaka, T. Shimoda, N. Takahashi, A. Shinohara, S. Wakamatsu, K. Katori, and H. Okamura, Phys. Rev. C **39**, 2268 (1989).

[22] D. J. Hofman, B. B. Back, and P. Paul, Phys. Rev. C **51**, 2597 (1995).

[23] H. Rossner, D. Hilscher, D. J. Hinde, B. Gebauer, M. Lehmann, M. Wilpert, and E. Mordhorst, Phys. Rev. C **40**, 2629 (1989).

[24] H. Rossner, D. J. Hinde, J. R. Leigh, J. P. Lestone, J. O. Newton, J. X. Wei, and S. Elfström, Phys. Rev. C **45**, 719 (1992).

[25] V. Weisskopf, Phys. Rev. **52**, 295 (1937).

[26] P. Fröbrich and I. I. Gontchar, Phys. Rep. **292**, 131 (1998).

[27] J. P. Lestone, Phys. Rev. Lett. **70**, 2245 (1993).

[28] A. V. Karpov, P. N. Nadtochy, D. V. Vanin, and G. D. Adeev, Phys. Rev. C **63**, 054610 (2001).

[29] J. Tian, N. Wang, and W. Ye, Phys. Rev. C **95**, 041601 (2017).

[30] I. Gontchar, L. Litnevsky, and P. Frbrich, Computer Physics Communications **107**, 223 (1997).

[31] W. Ye, Phys. Rev. C **81**, 054609 (2010).

[32] N. D. Mavlitov, P. Fröbrich, and I. I. Gonchar, Z. Phys. A **342**, 195 (1992).

[33] M. Brack, J. Damgaard, A. S. Jensen, H. C. Pauli, V. M. Strutinsky, and C. Y. Wong, Rev. Mod. Phys. **44**, 320 (1972).

[34] J. R. Nix, Nucl. Phys. A **130**, 241 (1969).

[35] K. T. R. Davies, A. J. Sierk, and J. R. Nix, Phys. Rev. C **13**, 2385 (1976).

[36] J. Sadhukhan and S. Pal, Phys. Rev. C **82**, 021601 (2010).

[37] W. Reisdorf, Z. Phys. A **300**, 227 (1981).

[38] A. V. Ignatyuk, M. G. Itkis, V. N. Okolovich, G. N. Smirenkin, and A. Tishin, Sov. J. Nucl. Phys. **21**, 612 (1975).

[39] A. J. Sierk, Phys. Rev. C **33**, 2039 (1986).

[40] W. D. Myers and W. J. Swiatecki, Nucl. Phys. **81**, 1 (1966).

[41] M. Blann, M. Beckerman, Nucleonika **23**, 34 (1978).

[42] M. Blann, Phys. Rev. C **21**, 1770 (1980).

[43] H. A. Bethe, Rev. Mod. Phys. **9**, 69 (1937).

[44] A. Bohr and B. Mottelson, *Nuclear Structure*, Vol. I (World Scientific, Singapore, 1975).

[45] W. Ye and N. Wang, Phys. Rev. C **87**, 014610 (2013).

[46] G. D. Adeev, A. V. Karpov, P. N. Nadtochii, and D. V. Vanin, Phys. Part. Nucl. **36**, 378 (2005).

[47] P. N. Nadtochy, G. D. Adeev, and A. V. Karpov, Phys. Rev. C **65**, 064615 (2002).

[48] J. Newton, D. Hinde, R. Charity, J. Leigh, J. Bokhorst, A. Chatterjee, G. Foote, and S. Ogaza, Nucl. Phys. A **483**, 126 (1988).